

## Application of bond energy model for different nanomaterials

Sandhya Bhatt\* & Munish Kumar

Department of Physics, G B Pant University of Agriculture and Technology, Pantnagar 263 145, India

Received 11 April 2017; accepted 21 July 2017

A simple theory has been developed using bond energy model of nanomaterials. The formulation has been obtained for the size and shape dependence of specific heat and conductivity. We have computed the size dependence of specific heat of Ag and Au nanoparticles. The results obtained have been compared with the available experimental data as well as with the earlier theoretical relation. It has been found that specific heat increases by decreasing the particle size. There is an appreciable improvement in the results as compared with the earlier relation and a good agreement with the available simulation data. We extend the model to study the effect of shape for the size dependence of specific heat and thermal conductivity of different nanomaterials. The results obtained have been discussed in the light of earlier investigations as well as experimental data. A good agreement between theory and experiment demonstrates the suitability of the formulation has been developed in the present paper.

**Keywords:** Bond energy model, Specific heat, Thermal conductivity, Size, Shape

### 1 Introduction

Nanostructure science and nanotechnology have become a multidisciplinary and one of the broadest fields of research in material science. Nanostructured materials include atomic clusters, layered films, thread like structures, and bulk nanocrystalline materials. Physics of nano scale materials is different from its macroscopic material and their properties are often superior due to which nanomaterials are of active research interest. By using different methods of synthesis, it is possible to tune their thermodynamic properties. These thermodynamic properties are influenced with the change of size as well as shape. Therefore, knowledge of these thermodynamic properties is necessary to design or fabricate them<sup>1</sup>. Thermodynamic properties like melting temperature, Debye temperature, specific heat, thermal conductivity etc. behave differently with the reduction of particle size<sup>2-4</sup>. Nanoscopic specific heat is a function of size, shape as well as temperature. Specific heat of Cu and Pd is about 10% and 40% higher as compared to their bulk values<sup>5</sup>. By studying Gibbs free energy of nanoparticles, Luo *et al.*<sup>6</sup> studied the thermodynamic properties of silver nanoparticles viz. melting temperature, molar heat of fusion, molar entropy of fusion and temperature dependence of entropy and specific heat. Studies reveal that these thermodynamic

properties can be divided into two parts; bulk quantity and surface quantity, and surface atoms dominate for the size effect on the thermodynamic properties of nanomaterials. The heat capacity of ideal nickel, copper, gold, aluminum and palladium FCC clusters with diameter up to 6 nm has been studied<sup>7</sup> in the temperature range of 150–800 K in terms of the molecular dynamics theory using a tight binding potential. This study shows an enhancement in specific heat at nanoscale.

Manufacturing and processing of a material require the knowledge of its thermal properties. Thermal conductivity of nanomaterial is affected by the temperature, size and shape. The thermal conductivity of single crystal of silicon has been measured<sup>8</sup> from 3 to 1580 K and of single crystal of germanium from 3 to 1190 K. These measurements have been made using a steady state, radial heat flow apparatus for  $T > 300$  K and a steady state longitudinal flow apparatus for  $T < 300$  K. This radiation flow technique eliminates thermal radiation losses at high temperatures. At all temperatures, major contribution of thermal conductivity in Si and Ge is produced by phonons. Thermal conductivity has been calculated from a combination of the relaxation times for boundary, isotope and phonon scattering and was found to agree with the experimental measurements. Above 700 K for Ge and 1000 K for Si, an electronic contribution to specific heat occurs, which agrees well with the

\*Corresponding author (E-mail: sandhyabhatt91@gmail.com)

theoretical estimates. Mante and Volger<sup>9</sup> measured the thermal conductivity of single crystalline BaTiO<sub>3</sub> in the temperature range 100–500 K. A reduction in the thermal conductivity has been observed. The results were explained in view of the theory based on the concept of low frequency ferroelectric modes of lattice vibration. Nath and Chopra<sup>10</sup> measured the thermal conductivity of thin films of copper and found a decrement with decreasing film thickness. An electrical thermal transport analogy has been used to calculate the size dependent thermal conductivity of thin copper films. It has been discussed that the decrease of thermal conductivity with thickness is attributed partly to the scattering of the conduction electrons from the film surfaces and partly to the scattering by lattice impurity. *Ab initio* simulation of lattice dynamics in semiconducting crystals has also been performed<sup>11</sup>. Yang *et al.*<sup>12</sup> observed a strong grain size dependent reduction in thermal conductivity at all temperatures from 6 – 480 K. It has been discussed that this behaviour is due to the effect of interfacial (kapitza) resistance on thermal transport. In response to the application of heat to a material, interfacial resistance results in a small temperature discontinuity at every grain boundary, an effect that is magnified in nanocrystalline materials because of the large number of grain boundaries. The thermal conductivities of individual single crystalline intrinsic Si nanowires with diameters of 22, 37, 56, and 115 nm have been measured<sup>13</sup> using a micro-fabricated suspended device over a temperature range of 20–320 K. The strong diameter dependence of thermal conductivity in nanowires was ascribed to the increased phonon-boundary scattering and possible phonon spectrum modification. A vapor deposition method (directed electron beam) has been used to grow yttria stabilized zirconia coatings<sup>14</sup> to study the substrate rotation effects upon the coating porosity, morphology, texture, and thermal conductivity. The thermal conductivity was found to be inversely related to the pore fraction. Thermal conduction in ultrathin silicon layers largely influences to nanoscale sensors and other thermo mechanical storage devices. The lateral thermal conductivity of single-crystal silicon layers (20 and 100 nm) has been measured using Joule heating and electrical-resistance thermometry<sup>2</sup> at temperatures between 20 and 300 K. A large reduction in thermal conductivity was found which is due to the phonon-boundary scattering at low temperatures. Diamond has the highest known room

temperature thermal conductivity but the integrated experimental and simulation study of thermal transport in ultra nanocrystalline diamond films<sup>15</sup> with a grain size of 3-5 nm showed a large reduction in thermal conductivity values. It was concluded that the grain boundaries have immanent properties to control this thermal transport. For face centered cubic crystal of Argon, phonon thermal conductivity has been predicted using the Boltzmann transport equation<sup>16</sup>. Boltzmann transport equation has also been used to predict the phonon thermal conductivities of argon and silicon thin films<sup>17</sup> under the relaxation time approximation by making use of potentials like Lenard-Jones for Argon and Stillinger-Weber for silicon. Studies on nano grained SrTiO<sub>3</sub> ceramics<sup>18</sup> show that thermal conductivity is a function of average grain size and decreases gradually with the drop in grain size. The prime factor is the presence of significant interface atoms acting as barriers for heat transport. The study also revealed that theoretical minimum conductivity could be achieved at an average grain size of about 10 nm. Flash method and four-point probe method have been used, respectively, to determine the grain-size dependent thermal conductivity and electrical resistivity of polycrystalline and nanocrystalline nickel<sup>19</sup>. The thermal conductivity of nanofluids containing dispersed silver nanoparticles of different sizes and volume fractions has been modeled<sup>20</sup>. Molecular dynamics simulation has been performed, using Voronoi tessellation method, for random grain shapes of nanocrystalline silicon<sup>21</sup>. Thermal conductivity has been calculated by the Green-Kubo method. Thermal conductivity of nanocrystalline silicon is far below its bulk value and increases quickly with increasing grain size. The effective phonon mean free path has been found as the main factor for such a large reduction in thermal conductivity at nanoscale. Studies of nano-grained strontium titanate (SrTiO<sub>3</sub>) films of varying grain-size, prepared from a chemical solution deposition process<sup>22</sup>, also results in reduction of thermal conductivity with decreasing average grain size and attributed in terms of increased phonon scattering at grain boundaries. The effect of grain size on thermal conductivity of thin film Barium titanate has been studied<sup>23</sup>. The findings of this study suggested that for complex oxide perovskites, thermal conductivity is driven by a spectrum of phonons with varying mean free paths. It has been demonstrated that size effects become stronger on grain boundary effects while measuring thermal conductivity at nanoscale.

Thus, a critical review of the literature shows that a lot of experimental work has been done related to the size dependence of specific heat and thermal conductivity. However, the theoretical efforts are lacking. Few efforts, based on potential approach or *ab initio* simulation made by earlier workers, are based on various approximations, involve tedious calculations and are time consuming. For example, it is a very difficult task, may be impossible, to extend the potential based approach for complicated solids. In the present paper, we therefore, develop a very simple and straightforward method to study the effect of size and shape, applicable for different type of solids, may be regarded as potential free approach. For this purpose, we used the bond energy model proposed by Qi<sup>24</sup>. The method developed introduces simplicity in complicated phenomena and is easily applicable for different solids.

**2 Theoretical Formulations**

Kumar and Kumar<sup>25</sup> used the bond energy model and studied the effect of size on cohesive energy, melting temperature and Debye temperature of nanomaterials. These authors reported the relation for Debye temperature of nanomaterials<sup>25</sup>, which reads as follows:

$$\theta_{Dn} = \theta_{Db} \left(1 - \frac{N}{2n}\right)^{1/2} \quad \dots (1)$$

where  $\theta_{Dn}$  and  $\theta_{Db}$  are the Debye temperatures of nanomaterial and bulk material respectively.  $N$  is the number of surface atoms and  $n$  the number of total atoms. Zhu *et al.*<sup>4</sup> discussed that the specific heat ( $C$ ) of bulk material is inversely proportional to the square of Debye temperature ( $C \propto 1/\theta_D^2$ ) and the approximation is valid for nanomaterials also. Singh *et al.*<sup>26</sup> used this approximation in Eq. (1) and obtained following relation for specific heat of nanomaterials (spherical shape):

$$C_n = C_b \left(1 - \frac{N}{2n}\right)^{-1} = \left(1 - \frac{2d}{D}\right)^{-1} \quad \dots (2)$$

The specific heat may be defined as:

$$C = \frac{dE}{dT} \quad \dots (3)$$

$$\text{or } E = C(T - T_0) \quad \dots (4)$$

where  $E$  is the cohesive energy and  $T_0$  is the reference temperature. In terms of the melting temperature ( $T_m$ ), Eq. (4) may be written as:

$$E_n = C_n (T_{mn} - T_0) \quad \dots (5)$$

$$\text{and } E_b = C_b (T_{mb} - T_0) \quad \dots (6)$$

The subscripts  $n$  and  $b$  refer to nano and bulk material, respectively. Using Eq. (5) and Eq. (6), we get the following relation:

$$\frac{C_n}{C_b} = \frac{E_n (T_{mb} - T_0)}{E_b (T_{mn} - T_0)} \quad \dots (7)$$

Equation (7) shows that the specific heat depends on cohesive energy and melting temperature. For this purpose, we used the bond energy model as critically reviewed by Qi<sup>27</sup>. According to this model, the cohesive energy of nanomaterial may be written as:

$$E_n = E_b \left(1 - \delta \frac{N}{n}\right) \quad \dots (8)$$

where  $\delta$  is the relaxation factor, which is defined as the ratio between the dangling bonds and total bonds of an atom. Assuming that the number of bonds is proportional to the surface area, one can write  $\delta = \frac{S_B}{S}$ ,

where  $S_B$  is the surface area with dangling bonds and  $S$  is the entire surface area of an atom. Qi<sup>27</sup> discussed different positions of the atom and reported that  $\delta$  may have the values  $1/4$ ,  $1/2$  and  $3/4$ . Thus, the relaxation factor is in the range  $0 \leq \delta < 1$ . We can thus rewrite Eq. (8) as follows:

$$E_n = E_b \left(1 - \frac{N}{4n}\right) \quad \dots (9)$$

$$E_n = E_b \left(1 - \frac{N}{2n}\right) \quad \dots (10)$$

$$E_n = E_b \left(1 - \frac{3N}{4n}\right) \quad \dots (11)$$

corresponding melting temperature reads as follows<sup>24,27</sup>:

$$T_{mn} = T_{mb} \left(1 - \frac{N}{4n}\right) \quad \dots (12)$$

$$T_{mn} = T_{mb} \left( 1 - \frac{N}{2n} \right) \quad \dots (13)$$

$$T_{mn} = T_{mb} \left( 1 - \frac{3N}{4n} \right) \quad \dots (14)$$

Putting these values of energy and melting temperature in Eq. (7), we get following relations for specific heat:

$$\frac{C_n}{C_b} = \left( 1 - \frac{N}{4n} \right) \left[ 1 - \frac{N}{4n} \left( \frac{T_{mb}}{T_{mb} - T_0} \right) \right]^{-1} \quad \dots (15)$$

$$\frac{C_n}{C_b} = \left( 1 - \frac{N}{2n} \right) \left[ 1 - \frac{N}{2n} \left( \frac{T_{mb}}{T_{mb} - T_0} \right) \right]^{-1} \quad \dots (16)$$

$$\frac{C_n}{C_b} = \left( 1 - \frac{3N}{4n} \right) \left[ 1 - \frac{3N}{4n} \left( \frac{T_{mb}}{T_{mb} - T_0} \right) \right]^{-1} \quad \dots (17)$$

It has already been discussed<sup>28</sup> that the value of  $N/n$  depends on the shape of material as given in Table 1. Thus, Eqs (15-17) can be written for different shapes of nanomaterials. For example, we write following relations for specific heat of spherical nanosolid:

$$\frac{C_n}{C_b} = \left( 1 - \frac{d}{D} \right) \left[ 1 - \frac{d}{D} \left( \frac{T_{mb}}{T_{mb} - T_0} \right) \right]^{-1} \quad \dots (18)$$

$$\frac{C_n}{C_b} = \left( 1 - \frac{2d}{D} \right) \left[ 1 - \frac{2d}{D} \left( \frac{T_{mb}}{T_{mb} - T_0} \right) \right]^{-1} \quad \dots (19)$$

$$\frac{C_n}{C_b} = \left( 1 - \frac{3d}{D} \right) \left[ 1 - \frac{2d}{D} \left( \frac{T_{mb}}{T_{mb} - T_0} \right) \right]^{-1} \quad \dots (20)$$

Similarly, we can write the relations of specific heat for different shapes of nanomaterials using the

Table 1 — Values of  $N/n$  and shape factor  $\alpha$  for different shapes<sup>28,29</sup>.

S. No.	Shape	$N/n$	$\alpha$
1	Film	(4/3) d/h	>1.15
2	Dodecahedral	1.796 d/a	1.09
3	Icosahedral	2.646 d/a	1.06
4	Wire	(8/3) d/L	>1.15
5	Sphere	4 d/D	1
6	Hexahedral	4 d/a	1.24
7	Octahedral	2√6 d/a	1.18
8	Tetrahedral	4√6 d/a	1.49

values of  $N/n$  corresponding to that shape. Thus, the present formulation is quite capable to include the effect of shape in addition to the size effect. A different model which includes the shape effects has also been developed by Qi and Wang<sup>29</sup>. In this model, the particle shape is considered by introducing a shape factor ( $\alpha$ ). According to this model, the relation for cohesive energy and melting temperature for nanosolids reads as follows (using the notations of present paper):

$$E_n = E_b \left( 1 - 3\alpha \frac{d}{D} \right) \quad \dots (21)$$

$$\text{and } T_{mn} = T_{mb} \left( 1 - 3\alpha \frac{d}{D} \right) \quad \dots (22)$$

Using Eqs (7), (21) and (22) we get:

$$\frac{C_n}{C_b} = \left( 1 - \frac{3\alpha d}{D} \right) \left[ 1 - \frac{3\alpha d}{D} \left( \frac{T_{mb}}{T_{mb} - T_0} \right) \right]^{-1} \quad \dots (23)$$

It has been discussed<sup>29</sup> that the shape factor for regular polyhedral ranges from 1 (sphere) to 1.49 (tetrahedral), where these two values provide the boundary limits for regular polyhedral nanoparticles (Table 1). Thus, for spherical<sup>29,30</sup> nanoparticles Eq. (23) reduces to Eq. (20). Some models of cohesive energy are inter-related as the surface area difference model<sup>30</sup>. The model simply gives the relation of cohesive energy as given by Eq. (9), which corresponds to  $\delta = 1/4$  in bond energy model. Thus, the relation obtained for specific heat using this model resembles with our Eq. (18). Qi<sup>27</sup> also generalized the above relation by using  $\frac{N}{n} = \frac{4\alpha d}{D}$ , which gives the following relation for cohesive energy and melting temperature:

$$E_n = E_b \left( 1 - \delta \frac{4\alpha d}{D} \right) \quad \dots (24)$$

$$\text{and } T_{mn} = T_{mb} \left( 1 - \delta \frac{4\alpha d}{D} \right) \quad \dots (25)$$

Further, using Eqs (7), (24) and (25), we get:

$$\frac{C_n}{C_b} = \left( 1 - \delta \frac{4\alpha d}{D} \right) \left[ 1 - \delta \frac{4\alpha d}{D} \left( \frac{T_{mb}}{T_{mb} - T_0} \right) \right]^{-1} \quad \dots (26)$$

For spherical nanoparticles with  $\delta = 3/4$ , Eq. (26) reduces to Eq. (20). Equations (2, 18-20) have been

used in the present paper to study the size dependence of specific heat for nanoparticles.

Now, we proceed to discuss the size and shape dependence of thermal conductivity of nanomaterials. The kinetic theory of solids gives following relation:

$$K_b = \frac{1}{3} C_b v_b l_b \quad \dots (27)$$

where  $K_b$  is the lattice thermal conductivity,  $v_b$  is the average phonon velocity and  $l_b$  is the mean free path.

Thus, we can write for nanomaterials:

$$K_n = \frac{1}{3} C_n v_n l_n \quad \dots (28)$$

Combining Eq. (27) and Eq. (28), we obtain:

$$\frac{K_n}{K_b} = \frac{C_n v_n l_n}{C_b v_b l_b} \quad \dots (29)$$

Singh *et al.*<sup>31</sup> assumed that specific heat in Eq. (29) is constant, i.e., independent of size, and reported the following relation for thermal conductivity (using the notations of present paper):

$$\frac{K_n}{K_b} = \left(1 - \frac{N}{2n}\right)^{3/2} \quad \dots (30)$$

It is very clear from above discussion that specific heat depends on size. Thus, it is legitimate and may be useful to include the size dependence of specific heat and modify Eq. (30) for thermal conductivity.

Liang and Li<sup>32</sup> discussed that the mean free path and melting temperature are related as follows:

$$\frac{l_n}{l_b} = \frac{T_{mn}}{T_{mb}} \quad \dots (31)$$

Combining Eq. (12) and Eq. (31), we get:

$$\frac{l_n}{l_b} = \left(1 - \frac{N}{4n}\right) \quad \dots (32)$$

$v_n$  and  $v_b$  may be written as follows<sup>33</sup>

$$\frac{v_n}{v_b} = \left(1 - \frac{N}{4n}\right)^{1/2} \quad \dots (33)$$

Now, in Eq. (29), using Eqs (15, 32, 33) gives the following relation:

$$\frac{K_n}{K_b} = \left(1 - \frac{N}{4n}\right)^{3/2} \left[1 - \frac{N}{4n} \left(\frac{T_{mb}}{T_{mb} - T_0}\right)\right]^{-1} \quad \dots (34)$$

Nan and Birringer<sup>34</sup> discussed the theory for effective thermal conductivity of a nanosolid based on kapitza resistance ( $R_k$ ) using effective medium approach. The theory was further improved by Yang *et al.*<sup>35</sup> assuming that the sharing of grain boundary region takes place between two grains. This gives the following relation<sup>35</sup>:

$$K = \frac{K_n}{1 + \frac{R_k K_n}{D}} \quad \dots (35)$$

These effects are included in the theory because the phonon mean free path is reduced due to increased phonon scattering effects in intragranular with decreasing grain size. Thus, the effective thermal conductivity of a nanosolid in terms of kapitza resistance can be written by using Eqs (34) and (35) as follows:

$$K = \frac{K_b \left(1 - \frac{N}{4n}\right)^{3/2} \left[1 - \frac{N}{4n} \left(\frac{T_{mb}}{T_{mb} - T_0}\right)\right]^{-1}}{1 + \frac{R_k K_b}{D} \left(1 - \frac{N}{4n}\right)^{3/2} \left[1 - \frac{N}{4n} \left(\frac{T_{mb}}{T_{mb} - T_0}\right)\right]^{-1}} \quad \dots (36)$$

Here  $N/n$  has the values as discussed above for different shapes of nanomaterials. Thus, Eq. (36) reported in the present paper, may be used to study the size as well as shape dependence of nanomaterials. On the basis of Eq. (26), we can also write the relation for thermal conductivity in terms of  $\alpha$  and  $\delta$  as given below:

$$K = \frac{K_b S}{1 + \frac{R_k K_b}{D} S} \quad \dots (37)$$

$$\text{where } S = \left(1 - \delta \frac{4\alpha d}{D}\right)^{3/2} \left[1 - \delta \frac{4\alpha d}{D} \left(\frac{T_{mb}}{T_{mb} - T_0}\right)\right]^{-1}$$

### 3 Results and Discussion

The properties of solids are related to the bonding energy between atoms, which are characterized by the cohesive energy. The properties of nanomaterials arise basically from their surface effect. To account

the surface effect, size, shape and relaxation must be considered. Based on core – shell structure, bond energy model has already been developed<sup>24</sup>. In this model, it is assumed that the cohesive energy of a solid consists of contributions from both surface and interior atoms. The application of bond energy model to predict size and shape dependent thermodynamic properties including its assumptions has been discussed by Qi<sup>27</sup>. In the present paper, we extended the bond energy model to obtain the formulations for the study of size and shape dependence of specific heat and thermal conductivity. Kumar and Kumar<sup>25</sup> reported the relation for the size dependence of Debye temperature. Under the approximation that specific heat is inversely proportional to the square of Debye temperature, Singh *et al.*<sup>26</sup> wrote the relation for specific heat (Eq. (2)). We extended the bond energy model and Eqs (18-20) based on different values of relaxation factor has been obtained as proposed by Qi<sup>27</sup>. It has already been discussed that the relaxation factor has different values ( $0 \leq \delta < 1$ ). We have selected the values of  $\delta$  at an interval of  $\frac{1}{4}$ .

Equations (2, 18-20) have been used to study the size dependence of specific heat of Ag and Au nanoparticles in spherical shape. We have selected these nanomaterials because of the fact that for these materials the simulation data<sup>6,7</sup> are available so that a comparison can be presented. The results are reported in Figs 1 and 2 along with the available simulation data. It is observed that Eq. (2) gives maximum deviations. These results are improved by Eq. (20). However, most of the simulation data lie in between the results predicted by Eq. (18) and Eq. (19). This

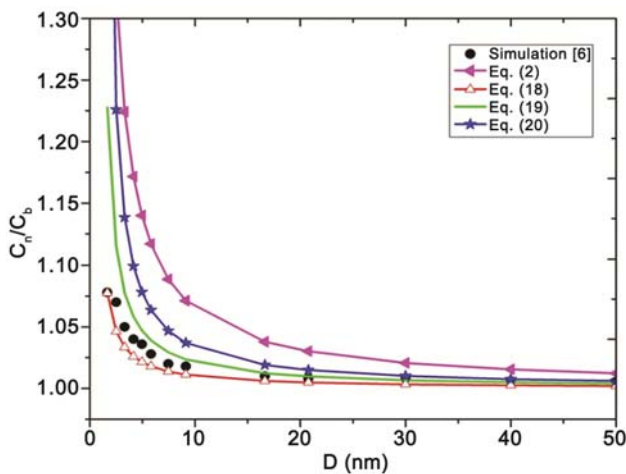


Fig. 1 — Size dependence of  $C_n/C_b$  for Ag (spherical) nanoparticle.

difference in the theoretical results may be within the simulation errors, not found in the literature<sup>6,7</sup>. It seems that for smaller particle size, the simulation data marching towards the results obtained by Eq. (18). However, for larger particle size, no significant difference is observed between the results obtained by Eq. (18) and Eq. (19). Thus, the above analysis seems to be good for the size dependence of specific heat which is found to increase by decreasing particle size. Moreover, the effect is very small for higher particle size. This enhancement at nano-scale may be due to the presence of surface atoms and high value of their atomic thermal vibration energy. Luo *et al.*<sup>6</sup> discussed this discrepancy between bulk and nanomaterials in terms of surface free energy. The model can also be used to study the effect of shape by using the values of  $N/n$  for desired shape as discussed in Table 1. We used Eq. (18) to study the effect of shape. The results obtained for Ag nanoparticles are reported in Fig. 3. It

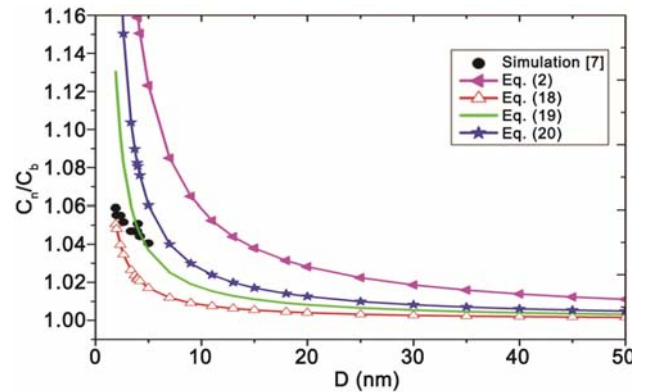


Fig. 2 — Size dependence of  $C_n/C_b$  for Au (spherical) nanoparticle.

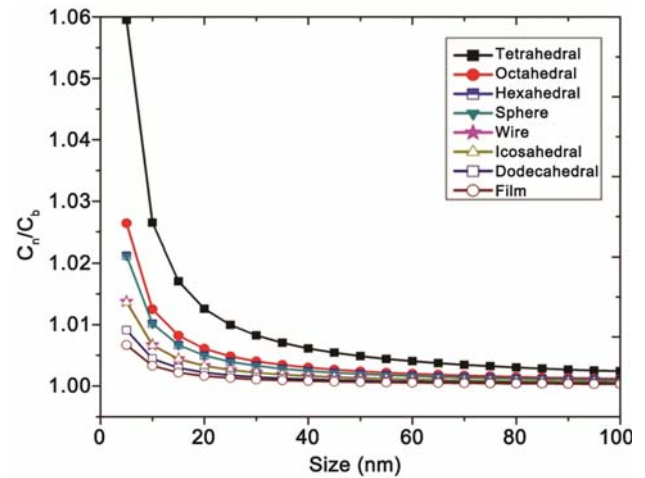


Fig. 3 — Size dependence of specific heat of Ag nanoparticle for different shapes using Eq. (18).

is found that  $C_n/C_b$  is highest for tetrahedral shape and minimum for film. For other shapes, the results lie between these two shapes.

To demonstrate a more critical test of the theory formulated in present paper, we extend our model (Eq. 18) to study the size dependence of thermal conductivity. Singh *et al.*<sup>31</sup> also reported the relation for the size dependence of thermal conductivity. These authors<sup>31</sup> assumed that specific heat is constant, and derived Eq. (30). We have studied the specific heat as discussed in the above section and also included the recent studies related to the specific heat by Singh *et al.*<sup>26</sup>. These studies demonstrate very clearly that specific heat is not constant as assumed earlier<sup>31</sup>. In the present paper, we considered the size dependence of specific heat as given by Eq. (18) and obtained Eq. (36). Thus, Eq. (36) may be regarded as the modified form of Eq. (30) in the sense that Eq. (36) is based on the fact that specific heat depends on the size whilst in Eq. (30) specific heat has been assumed to be constant. In the present paper, we used both the equations to study the size dependence of thermal conductivity. The results obtained are reported in Figs 4-6 along with the available simulation and experimental data. We have considered different shapes of nanomaterial, viz., spherical, nanowire and nanofilm, according to the availability of the earlier data so that a comparison can be made. Size dependent thermal conductivity of Si (spherical) computed using Eq. (30) and Eq. (36) is reported in Fig. 4 along with the simulation data<sup>3,21</sup>. For the larger size (above 20 nm), Eq. (30) shows that thermal conductivity is almost constant, while for

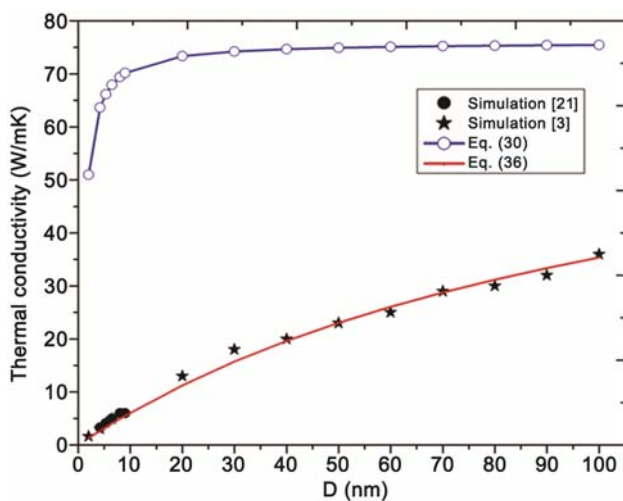


Fig. 4 — Size effect on thermal conductivity of Si (spherical) nanoparticle at 500 K.

smaller size (below 20 nm) there is a sharp decrease with decreasing particle size. However, this behaviour is neither observed in the computed values from Eq. (36) nor in the simulation data. It is found that Eq. (30) deviates largely while the results obtained from Eq. (36) are in good agreement with the experimental data<sup>3,21</sup>. The computed values of size dependence of thermal conductivity using Eq. (30) and Eq. (36) are reported in Fig. 5 for Si (nanowire) along with the available experimental data<sup>13</sup>. It is found that the results obtained by Eq. (36) agree well with the experimental findings as compared with Eq. (30).

Liu and Asheghi<sup>2</sup> measured the thermal conductivity and wrote “The thermal conductivity of 20 nm thick silicon layer is ~ 22 W/mK.” We have therefore selected Si (thin film) of size 20 nm for comparison purpose. Thermal conductivity computed using Eq. (36) gives 23.4 W/mK. These results are

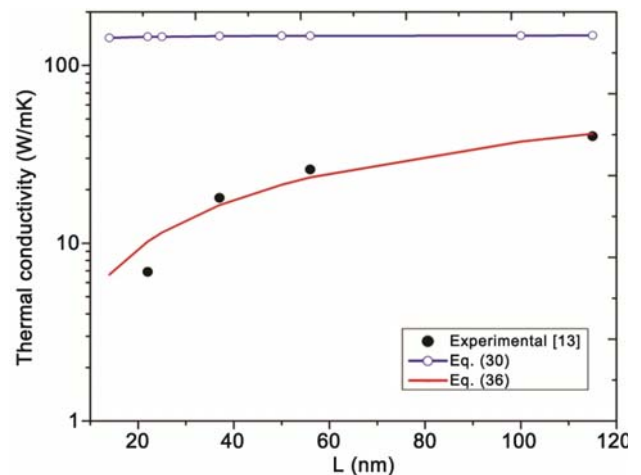


Fig. 5 — Size effect on thermal conductivity of Si (nanowire).

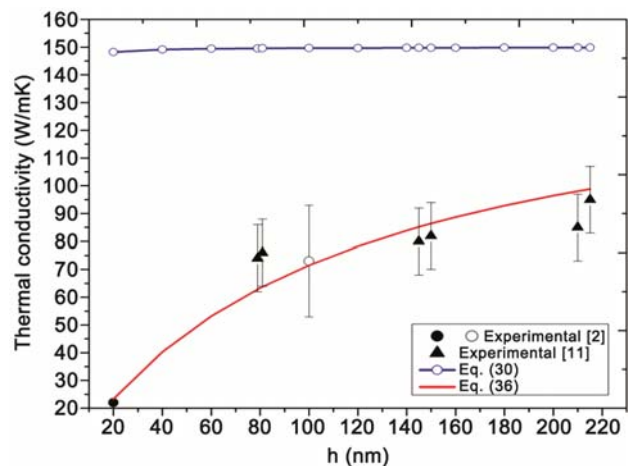


Fig. 6 — Size effect on thermal conductivity of Si (nanofilm).

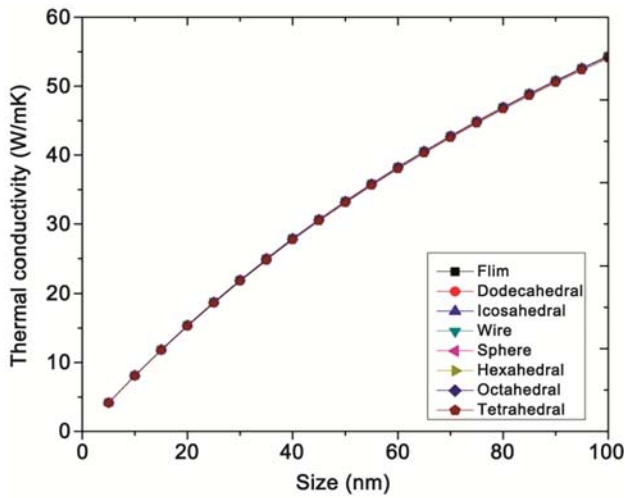


Fig. 7 — Size dependence of thermal conductivity of Si nanomaterial for different shapes using Eq. (36).

Table 2 — Input data used in present paper<sup>36</sup>.

Nanomaterial	$d$ (nm)	$T_{mb}$ (K)	$K_b$ (W/mK)
Ag	0.304	1235	—
Au	0.274	1338	—
Si	0.234	1687	148

reported in Fig. 6. The required input data<sup>36</sup> are given in Table 2. The  $R_k$  values are obtained from non linear least square fitting of corresponding experimental or simulation data. We used Eq. (36) to study the shape dependence of thermal conductivity of Si nanomaterial for different shapes using  $R_k$  as shape independent which is  $1.16 \times 10^{-9} \text{ m}^2 \text{ KW}^{-1}$  as reported by Ju and Liang<sup>37</sup>. The results obtained are reported in Fig. 7. It is observed that there is a very little effect of shape on thermal conductivity of Si nanomaterial using  $R_k$  as shape independent.

#### 4 Conclusions

We developed a simple formulation based on bond energy model to understand the size and shape dependence of specific heat and thermal conductivity. It is found that specific heat increases whereas thermal conductivity decreases with decreasing particle size. The results obtained are compared with the earlier investigations as well as simulation and experimental data. A good agreement between theory and experiment supports the validity of the formulation developed.

#### Acknowledgement

One of the authors S B is thankful to Department of Science and Technology, New Delhi, India for financial support in the form of INSPIRE fellowship.

#### References

- Xiong S, Qi W H, Cheng Y, Huang B, Wang M P & Li Y, *Phys Chem Chem Phys*, 13 (2011) 10652.
- Liu W & Asheghi M, *Appl Phys Lett*, 84 (2004) 3819.
- Dong H, Wen B & Melnik R, *Nature Sci Rep*, 4 (2014) 7037.
- Zhu Y F, Lian J S & Jiang Q, *J Phys Chem C*, 113 (2009) 16896.
- Rupp J & Birringer R, *Phys Rev B: Condens Matter*, 36 (1987) 7888.
- Luo W H, Hu W Y & Xiao S F, *J Phys Chem C*, 112 (2008) 2359.
- Gafner Y Y, Gafner S L, Zamulin I S, Redel L V & Baidyshev V S, *Phys Met Metallogr*, 116 (2015) 568.
- Glassbrenner C & Slack G A, *Phys Rev*, 134 (1964) A1058.
- Mante A J H & Volger J, *Phys Lett A*, 24 (1967) 139.
- Nath P & Chopra K L, *Thin Solid Films*, 20 (1974) 53.
- Ju Y S & Goodson K E, *Appl Phys Lett*, 74 (1999) 3005.
- Yang H S, Eastman J A, Thompson L J & Bai G R, *Mater Res Soc Proc*, 703 (2001) V4.7.
- Li D, Wu Y, Kim P, Shi L, Yang P & Majumdar A, *Appl Phys Lett*, 83 (2003) 2934.
- Zhao H, Yu F, Bennett T D & Wadley H N G, *Acta Mater*, 54 (2006) 5195.
- Angadi M A, Watanabe T, Bodapati A, Xiao X, Auciello O, Carlisle J A, Eastman J A, Keblinski P, Schelling P K & Phillpot S R, *J Appl Phys*, 99 (2006) 114301.
- McGaughey A J H & Kaviani M, *Phys Rev B*, 69 (2004) 094303.
- Turney J E, McGaughey A J H & Amon C H, *J Appl Phys*, 107 (2010) 024317.
- Wang Y, Fujinami K, Zhang R, Wan C, Wang N, Ba Y & Koumoto K, *Appl Phys Express*, 3 (2010) 031101.
- Wang S, Master Thesis, Graduate Department of Materials Science and Engineering, University of Toronto, 2011.
- Warrier P & Teja A, *Nanoscale Res Lett*, 6 (2011) 247.
- Ju S & Liang X, *J Appl Phys*, 112 (2012) 064305.
- Foley B M, Shaklee H J B, Duda J C, Cheaito R, Gibbons B J, Medlin D, Ihlefeld J F & Hopkins P E, *Appl Phys Lett*, 101 (2012) 231908.
- Donovan B F, Foley B M, Ihlefeld J F, Maria J P & Hopkins P E, *Appl Phys Lett*, 105 (2014) 082907.
- Qi W H, *Physica B*, 368 (2005) 46.
- Kumar R & Kumar M, *Indian J Pure Appl Phys*, 50 (2012) 329.
- Singh M, Lara S & Tlali S, *J Taibah Univ Sci*, 11 (2017) 922.
- Qi W H, *Acc Chem Res*, 49 (2016) 1587.
- Bhatt S & M Kumar, *J Phys Chem Solids*, 106 (2017) 112.
- Qi W H & Wang M P, *Mater Chem Phys*, 88 (2004) 280.
- Qi W H & Wang M P, *J Mater Sci Lett*, 21 (2002) 1743.
- Singh M, Hlabana K K, Singhal S & Devlal K, *J Taibah Univ Sci* 10 (2016) 375.
- Liang L H & Li B, *Phys Rev*, 73 (2006) 153303.
- Regel A R & Glazov V M, *Semiconductors*, 29 (1995) 405.
- Nan C W & Birringer R, *Phys Rev B*, 57 (1998) 8264.
- Yang H S, Bai G R, Thompson L J & Eastman J A, *Acta Mater*, 50 (2002) 2309.
- Kittel C, *Introduction to solid state physics*, 8th ed. (John Wiley and Sons Inc), 2013.
- Ju S & Liang X, *J Appl Phys*, 112 (2012) 064305.